

Stability of free planar films of liquid ^4He at $T=0$ K

Leszek Szybisz*

Laboratorio TANDAR, Departamento de Física, Comisión Nacional de Energía Atómica, Av. del Libertador 8250, RA-1429 Buenos Aires, Argentina
and Departamento de Física, Facultad de Ciencias Exactas y Naturales, Universidad de Buenos Aires, Ciudad Universitaria, RA-1428 Buenos Aires, Argentina

(Received 4 February 1997; revised manuscript received 1 July 1997)

The stability of planar films of liquid ^4He at $T=0$ K without a supporting potential is investigated. For this purpose, the third-sound velocity, c_3 , is examined within the framework of two different theoretical descriptions: (i) the correlated-basis functions theory in conjunction with the hypernetted-chain approximation and (ii) the nonlocal density functional theory. All the calculations yield negative values of c_3^2 . In particular, the behavior of the chemical potential as a function of the coverage provides convincing evidence in favor of the instability of all the analyzed free films. Furthermore, the analysis of the trend of thick films leads to the plausible conjecture that free planar films with finite coverage would be always unstable. The conclusion of the present work matches well with the nonwetting phenomenon of Rb and Cs substrates by a liquid ^4He film at $T=0$ K and with the hydrodynamic prediction that a free semi-infinite system with a flat surface is unstable. [S0163-1829(97)03141-X]

I. INTRODUCTION

In recent years much work has been devoted in order to study planar helium films by performing both experiments and theoretical developments. In this geometry the liquid is translationally invariant in the x - y plane and exhibits a density profile in the z direction. To get an insight into the different theoretical approaches for tackling this problem the reader is referred to the review article of Cheng *et al.*¹

The investigation of the stability of Bose helium films at $T=0$ K is perhaps one of the most interesting issues in this field. The condition for having a stable geometry is related to the third-sound velocity. Third sound is a long-wavelength surface perturbation which is propagated parallel to the liquid-vacuum interface of the helium film like a tidal wave on the ocean. The speed of propagation of this disturbance is denoted as c_3 . The stability condition for a film of finite surface coverage n_c requires that c_3 be positive. The surface coverage is the number of particles per unit area

$$n_c = \frac{N}{A} = \int_{-\infty}^{\infty} dz \rho(z), \quad (1.1)$$

where $\rho(z)$ is the density profile as a function of the coordinate z perpendicular to the surface. The third-sound velocity may be calculated either from the long-wavelength limit of the ripplon excitation energy at a fixed n_c or from the behavior of the chemical potential as a function of n_c . Explicit formulas to evaluate c_3 are given in a next section.

Within the general problem of the stability of inhomogeneous Bose quantum systems, the behavior of free films of liquid ^4He at zero absolute temperature deserves particular attention. Although a self-supporting fluid with translationally invariant x - y planar symmetry does not exist in nature, it is still relevant to know properties of such rather academic systems. The interest is mainly due to two reasons. On the

one hand, this special kind of system may be considered as the limiting case of very weak external potentials and, on the other hand, very thick free films should tend to exhibit features of the bulk liquid.

Let us now put the case of free planar films in the context of the current state of the art concerning the study of the stability of inhomogeneous liquid ^4He . In a pioneering work, Widom has shown within the hydrodynamic theory of surface tension that a semi-infinite ^4He system with a free planar surface is unstable.² Subsequently, Cole has demonstrated that this instability can be removed by including a gravitational term.³ In both these papers the microscopic structure of the liquid was ignored. After the dramatic improvement of computational facilities microscopic theories have been applied to carry out self-consistent calculations for inhomogeneous liquid ^4He . In the present work we shall refer to two of these approaches. One of them is an *ab initio* variational method based on the theory of correlated-basis functions (CBF's) proposed by Feenberg⁴⁻⁶ which is employed in conjunction with the hypernetted-chain (HNC) expansion. Within this framework the structure and excitation spectra of liquid ^4He films at $T=0$ K could be satisfactorily interpreted.⁷⁻²³ The CBF-HNC approach has also been successfully applied to analyze semi-infinite systems of liquid ^4He at zero absolute as well as at finite temperature.²⁴⁻³⁰ The other procedure which we shall introduce is the nonlocal density functional (NLDF) theory developed on the basis of the density functional model proposed by Saam and Ebner.^{31,32} The NLDF method reported by Dupont-Roc *et al.*³³ has been used to calculate several properties of ^4He films.³⁴⁻³⁸ In the following lines we shall focus our attention on results of the studies of helium systems adsorbed to surfaces. For instance, Clements *et al.*^{16-19,23} investigated the growth of ^4He films adsorbed to attractive substrates by using the CBF-HNC expansion. This microscopic theory has a "built in" consistency test in the sense that the corresponding Euler-Lagrange (EL) equations cease to have solutions if

the assumed geometry of the system under consideration is unstable against infinitesimal density fluctuations. To this respect, it is well known that for a uniform ${}^4\text{He}$ liquid the EL equation does not give (unphysical) solutions if one attempts to solve the system at a density lower than the *spinodal density* where the compressibility becomes negative.^{5,6,39} The authors of Refs. 16–19 and 23 found that EL equations do not have solutions for all surface coverages n_c . Figure 2 of Ref. 16 clearly shows that only in some well-defined regimes of coverage the third-sound velocity is positive. Quantity c_3 becomes imaginary between stable domains indicating regions of instability, the first of which occurs for $0 < n_c < n_c^{\min}$ when the film just begins to grow. The latter result is in agreement with a previous remark of Cheng *et al.*,³⁵ who pointed out that a remarkable feature of ${}^4\text{He}$ films is that for any substrate there is a minimum stable coverage n_c^{\min} below which the adsorbed systems are unstable. In the literature it is frequent to say that ${}^4\text{He}$ wets a certain substrate when the adsorbed helium forms a stable film.

For our purpose, it becomes illuminating to look carefully at the feature that films supported by substrate potentials $U_{\text{sub}}(z)$ can be unstable at certain regimes of surface coverage. In order to explore the sensitivity of this behavior to the actual shape of the external field, Clements and collaborators^{16–18} have carried out calculations varying both the *well depth* and the *range* of the substrate potential, which frequently obeys the form $U_{\text{sub}}(z) = B/z^9 - C/z^3$. A comparison among interaction potentials for a ${}^4\text{He}$ atom above different substrates is shown in Fig. 4 of Ref. 18. They concluded that less attractive potentials lead to larger domains of instability (see, e.g., Fig. 12 in Ref. 17) and, in addition, found that stability depends significantly on the *range* of $U_{\text{sub}}(z)$ determining that shorter-ranged potentials also tend to yield more extended regions of instability.^{17,18} From these results one can infer that for very short-ranged potentials with smaller and smaller strength the unstable domains will dominate the whole pattern. Furthermore, by extrapolating this tendency to the extreme limit corresponding to the absence of any external potential, $U_{\text{sub}}(z) \equiv 0$, one could conjecture that in such a case the stable regions would finally disappear completely. In fact, this trend has already been observed in calculations carried out for alkali-metal surfaces by using the NLDF theory. In particular, it was predicted^{35,36} that ${}^4\text{He}$ should not wet substrates of heavy alkali metals like K, Rb, and Cs which generate attractive adsorbate-substrate potentials weaker than that corresponding to a ${}^4\text{He}$ “substrate” (see, e.g., Fig. 1 in Ref. 1). This prediction has been supported by subsequent variational Monte Carlo calculations⁴⁰ and the nonwetting of ${}^4\text{He}$ on rubidium and cesium at $T = 0$ K has already been confirmed by a few experimental groups.^{41–45}

In fact, free planar films of helium have been already investigated^{7,8,11} by applying the CBF-HNC expansion and the question related to their stability has been also analyzed in this approach.^{11,13} However, from the discussions of the latter papers emerges a discrepancy. While our study of ripplon excitation energies provided some evidence for the instability of finite free films,¹¹ Krotscheck and Tymczak¹³ criticized the meaning of our finding. They stated that our results might be influenced by numerical uncertainties and

claimed that such systems are stable since there is no clear indication for the contrary. Of course, an argument based exclusively on the rejection of calculated values is not strong enough to ensure unambiguously stability. On the other hand, if non-very-thick planar free films were stable, while the same systems adsorbed to Rb and Cs surfaces are not, we would be faced with an *a priori* striking feature.

From the scenario described above, it becomes relevant to know whether films without a supporting substrate are stable or not. In view of the importance of this question and the rather confused situation arisen from Refs. 11 and 13, it turns out to be worthwhile to devote some effort in order to clarify the posed controversy establishing definitively the actual behavior of such systems. Therefore, the aim of the present work is just to review the issue concerning the stability of self-supported planar films of liquid ${}^4\text{He}$ at zero absolute temperature. In this doing, we shall first summarize and complete the analysis within the CBF-HNC expansion. Next, we shall solve the problem using the NLDF theory to allow a comparison of results provided by different approaches. This paper is organized as follows. In Sec. II the stability conditions are outlined. The discussion of the numerical results is presented in Sec. III. Section IV provides our conclusions.

II. STABILITY CONDITIONS

Before summarizing the stability conditions, we shall mention that in the case of a planar geometry any one-body function satisfies $f(\mathbf{r}) = f(z)$ and any two-body quantity $f(\mathbf{r}_1, \mathbf{r}_2)$ depends only on three variables: (i) the z coordinate of each of the two particles, i.e., z_1 and z_2 and (ii) the distance between both particles $r_{12} = |\mathbf{r}_2 - \mathbf{r}_1|$ projected onto the x - y plane, i.e.,

$$\eta = \eta_{12} = |\boldsymbol{\eta}_{12}| = |\boldsymbol{\eta}_2 - \boldsymbol{\eta}_1| = \sqrt{(x_2 - x_1)^2 + (y_2 - y_1)^2}, \quad (2.1)$$

so that any two-body function may be expressed as $f(\eta, z_1, z_2)$. Due to the planar symmetry sometimes it becomes useful to write formulas in terms of two-body quantities $\tilde{f}(q, z_1, z_2)$ which are Hankel transforms of the corresponding $f(\eta, z_1, z_2)$ evaluated according to

$$\begin{aligned} \tilde{f}(q, z_1, z_2) &= \sqrt{\rho(z_1)\rho(z_2)} \int f(\eta, z_1, z_2) \\ &\quad \times \exp[i(q_x x + q_y y)] dx dy \\ &= 2\pi \sqrt{\rho(z_1)\rho(z_2)} \int_0^\infty \eta d\eta J_0(\eta q) f(\eta, z_1, z_2), \end{aligned} \quad (2.2)$$

wherein J_0 is the zeroth-order Bessel function of the first kind. Here q is the momentum parallel to the surface. The distance between two particles is

$$r_{12} = |\mathbf{r}_2 - \mathbf{r}_1| = \sqrt{\eta_{12}^2 + (z_2 - z_1)^2} = \sqrt{\eta^2 + (z_2 - z_1)^2}. \quad (2.3)$$

In order to check the stability of a film one must calculate the third-sound velocity, which is conveniently expressed as

an energy mc_3^2 , where m is the atomic mass of ^4He . As already mentioned in the Introduction, there are two ways of evaluating mc_3^2 . We shall first refer to that based on the calculation of the ripplon energy at very small momenta q

for a film with fixed n_c . The stability condition derived in Ref. 11 has been written in terms of solutions of the excitation spectrum determined by the eigenvalue equation of the Bogoliubov-type derived in Ref. 7:

$$H^2(q, z_1)\psi_\kappa(q, z_1) + 2 \int_{-\infty}^{\infty} dz_2 \tilde{V}_{p-h}(q, z_1, z_2) H(q, z_2) \psi_\kappa(q, z_2) = \hbar^2 \omega_\kappa^2(q) \psi_\kappa(q, z_1), \quad (2.4)$$

and by the adjoint eigenvalue equation to Eq. (2.4) introduced in¹¹

$$H^2(q, z_1) \psi_\kappa^\dagger(q, z_1) + 2 \int_{-\infty}^{\infty} dz_2 [H(q, z_1) \tilde{V}_{p-h}(q, z_1, z_2)] \psi_\kappa^\dagger(q, z_2) = \hbar^2 \omega_\kappa^2(q) \psi_\kappa^\dagger(q, z_1), \quad (2.5)$$

where

$$H(q, z) = \frac{\hbar^2}{2m} \left(q^2 - \frac{1}{\sqrt{\rho(z)}} \frac{d}{dz} \rho(z) \frac{d}{dz} \frac{1}{\sqrt{\rho(z)}} \right), \quad (2.6)$$

and $\tilde{V}_{p-h}(q, z_1, z_2)$ is the Hankel transform (2.2) of the ‘‘particle-hole’’ potential $V_{p-h}(\eta, z_1, z_2)$ defined by Eq. (A4) in the Appendix of Ref. 21. The quantity $\hbar \omega_\kappa(q)$ is the energy of the excitation modes $\psi_\kappa(q, z)$ and $\psi_\kappa^\dagger(q, z)$ labeled by quantum number κ . A stable system requires a positive ripplon energy (mode with $\kappa=0$) for $q \rightarrow 0$

$$\hbar^2 \omega_0^2(q \rightarrow 0) = \frac{\hbar^2 q^2}{2m} \frac{h_0^\dagger(q \rightarrow 0)}{N_0^2(q \rightarrow 0)} = c_3^2 \hbar^2 q^2 > 0, \quad (2.7)$$

where $h_0^\dagger(q)$ is the matrix element

$$h_0^\dagger(q) = e_0^\dagger(q) + 2V_0^\dagger(q) = \int_{-\infty}^{\infty} dz_1 \psi_0^\dagger(q, z_1) H(q, z_1) \psi_0^\dagger(q, z_1) + 2 \int_{-\infty}^{\infty} \int_{-\infty}^{\infty} dz_1 dz_2 \psi_0^\dagger(q, z_1) \tilde{V}_{p-h}(q, z_1, z_2) \psi_0^\dagger(q, z_2), \quad (2.8)$$

and $N_0(q)$ is the generalized orthonormalization integral

$$N_0(q) = \int_{-\infty}^{\infty} dz_1 \psi_0(q, z_1) \psi_0^\dagger(q, z_1). \quad (2.9)$$

From Eq. (2.7) one gets the requirement

$$mc_3^2 = \frac{1}{2} \frac{h_0^\dagger(q \rightarrow 0)}{N_0^2(q \rightarrow 0)} > 0. \quad (2.10)$$

Since $N_0^2(q \rightarrow 0)$ is positive, to have a real third-sound velocity the inequality $h_0^\dagger(q \rightarrow 0) > 0$ must be satisfied.

The other procedure to determine mc_3^2 relies on the analysis of the variation of the chemical potential μ as a function of the coverage. The quantity μ is obtained from the Hartree-like equation which also determines the square root of the density profile

$$\left[-\frac{\hbar^2}{2m} \frac{d^2}{dz^2} + U_{\text{sub}}(z) + V_H(z) \right] \sqrt{\rho(z)} = \mu \sqrt{\rho(z)}. \quad (2.11)$$

Here $V_H(z)$ is a Hartree mean-field potential; its explicit expression depends on the adopted theoretical model. Cheng and collaborators have demonstrated within the NLDF theory that c_3 is related to the derivative of μ with respect to n_c . These authors derived the stability condition (see the Appendix of Ref. 36)

$$mc_3^2 = n_c \left(\frac{d\mu}{dn_c} \right) > 0. \quad (2.12)$$

Subsequently, Krotscheck and Tymczak¹³ have shown that condition (2.12) is also sufficient to guarantee stability in the CBF-HNC framework. However, within the latter approach the speed of the third sound calculated with Eqs. (2.10) and (2.12) will normally agree only for an exact expansion.¹⁸

III. ANALYSIS OF THE STABILITY

A. Evidence from the ripplon excitation energy

We shall first focus our attention on the numerical results concerning the stability test based on the evaluation of the third-sound velocity from the ripplon excitation energy in the limit of very small momentum q . Equations (2.8) and (2.10) indicate that, in order to have a stable system the matrix element $h_0^\dagger(0^+) = \langle H(0^+) + 2\tilde{V}_{p-h}(0^+) \rangle_0$ (here 0^+ stands for $q \rightarrow 0$) must be positive defined. In a previous work we have calculated $h_0^\dagger(0^+)$ for free symmetric films of liquid ^4He at $T=0$ K assuming that atoms interact via a standard 6-12 Lennard-Jones potential. The obtained values are listed in Table II of Ref. 11 and all of them are negative. Unfortunately, those results cannot be compared to others since in Refs. 7 and 8 there are no numerical data of mc_3^2 (from Figs. 1 and 3 of the latter paper it is impossible to get any precise information for $q \rightarrow 0$). Although our data have not been contrasted with other evaluations, they were criticized in the literature¹³ and their implication was disregarded. In order to make clear the grounds for such a criticism, we shall describe the context in which it is formulated. As is well known, the matrix element $\langle H(0^+) + 2\tilde{V}_{p-h}(0^+) \rangle_0$ goes to zero in the limit of large coverage due to a cancellation effect.²⁵ In particular, the evaluation of $\tilde{V}_{p-h}(q, z_1, z_2)$ at small momenta q becomes numerically very delicate. Such a cancellation is still operative to an important extent at finite coverages affecting the calculation of the long-wavelength limit of required matrix elements. In view of these facts, Krotscheck and Tymczak¹³ suggested that our values of $h_0^\dagger(0^+)$ calculated from ripplon excitations in Ref. 11 might be negative due to possible computational uncertainties caused by the above-mentioned cancellation effect rather than to real physical reasons. The authors of Ref. 13 concluded stating that our results cannot be utilized to draw any conclusion about the stability question. So one has to recourse to an alternative way to settle this controversial situation.

B. Evidence from the chemical potential

If one disregards the indication for instability appearing intrinsically in the CBF-HNC calculational scheme, then the unique way to gain insight into the stability of a finite system of liquid ^4He at $T=0$ K is to analyze the behavior of $d\mu/dn_c$. In practice, Krotscheck and co-workers^{10,13,16-18} as well as Cheng and collaborators^{1,35-38} have explored the behavior of the derivative $d\mu/dn_c$ in order to get information about mc_3^2 in confined systems. Following such a procedure we shall now examine the variation of the chemical potential as a function of n_c in the case of free planar films. This investigation is done in two steps: first we complete and analyze data provided by the CBF-HNC expansion; second, we calculate μ applying the NLDF theory and examine its behavior.

1. Chemical potential in the CBF-HNC expansion

This section is devoted to analyze the data of μ listed in Table I of Ref. 7 and in Table II of Ref. 11. Both these sets of μ were obtained in the CBF-HNC/0 approximation [i.e.,

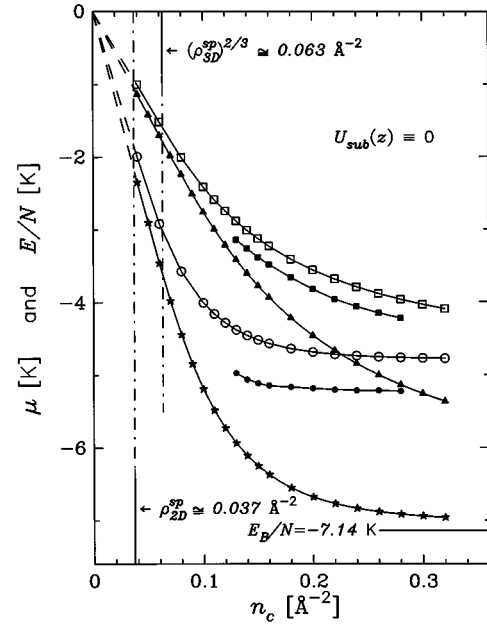


FIG. 1. Chemical potential and energy per particle as a function of the coverage. Results obtained with the CBF-HNC/0 expansion are indicated by circles (chemical potential) and squares (energy per particle). In this case open symbols stand for the short-ranged values calculated in the present work, while full symbols are the optimized results taken from Table I of Ref. 7. Full triangles and stars are, respectively, the chemical potential and the energy per particle evaluated using the NLDF theory. The vertical lines indicate the two-dimensional spinodal density ρ_{2D}^{sp} and the equivalent surface density $(\rho_{3D}^{sp})^{2/3}$ of the three-dimensional spinodal value $\rho_{3D}^{sp} \approx 0.0158 \text{ \AA}^{-3}$.

neglecting the contribution of all elementary diagrams as pointed out when discussing Eqs. (2.6)–(2.8) in Ref. 11]. The difference is due to the fact that the calculations were carried out by assuming different potentials to account for the interaction between helium atoms. As mentioned before, the standard 6-12 Lennard-Jones potential was used in Ref. 11, while in Ref. 7 the Aziz⁴⁶ potential was utilized. The values of Ref. 7 are plotted in Fig. 1. In a discussion of these results Krotscheck and Tymczak¹³ suggested that free planar films are stable because even though the calculated $\mu(n_c)$ yield a small negative slope they suspect that such a negative value is not large enough to indicate a real instability of the equations. However, no evaluation of the slope illustrates their statement. Since in order to establish unambiguously that a numerical result is negligibly small one should perform an appropriate comparison, a claim like the one transcribed above cannot be taken as a final asseveration. Therefore, we have undertaken a search for the physical content of these optimized values of μ by adopting a more comprehensive perspective, which includes an estimation of the expected slope.

According to the idea outlined in the previous paragraph, the first step was to evaluate a set of values of μ for the planned comparison. Our experience in the study of this kind of film indicates that results obtained by solving the system assuming short-ranged correlations provide a good reference for meaningful comparisons (see, e.g., trends of short-ranged and optimized solutions in Table II and Figs. 5, 9, and 10 of

Ref. 11). So we solved free films of liquid ${}^4\text{He}$ at $T=0$ K by using short-ranged correlation factors of the generalized McMillan-Schiff-Verlet type introduced in Ref. 11:

$$u(\eta, z_1, z_2) = - \left(\frac{b_0 + b_1 \sqrt{\rho(z_1)\rho(z_2)}}{\sqrt{\eta^2 + (z_1 - z_2)^2}} \right)^5 \quad (3.1)$$

with $b_0 = 2.8 \text{ \AA}$ and $b_1 = 9.98 \text{ \AA}^4$. It is worthwhile to mention that Carraro and Cole have also utilized a sort of McMillan-Schiff-Verlet correlation factor in a variational

Monte Carlo evaluation of the binding energy of ${}^4\text{He}$ films on several alkali-metal substrates.⁴⁰ The CBF-HNC/0 calculations were performed by adopting for $V_H(z)$ the formula derived by Saarela *et al.*²⁴

$$V_H(z_1) = \int_{-\infty}^{\infty} dz_2 \rho(z_2) [2E_c(z_1, z_2) + E_{NX}(z_1, z_2)], \quad (3.2)$$

where

$$E_c(z_1, z_2) = \pi \int_0^{\infty} \eta d\eta \left(g(\eta, z_1, z_2) v(r_{12}) + \frac{\hbar^2}{2m} [|\nabla_1 \sqrt{g(\eta, z_1, z_2)}|^2 + |\nabla_2 \sqrt{g(\eta, z_1, z_2)}|^2] - \frac{\hbar^2}{8m} [\nabla_1 g(\eta, z_1, z_2) \cdot \nabla_1 N(\eta, z_1, z_2) + \nabla_2 g(\eta, z_1, z_2) \cdot \nabla_2 N(\eta, z_1, z_2)] \right), \quad (3.3)$$

and

$$E_{NX}(z_1, z_2) = - \frac{\pi \hbar^2}{8m} \int_0^{\infty} \eta d\eta [\nabla_2 N(\eta, z_1, z_2) \cdot \nabla_2 X(\eta, z_1, z_2)]. \quad (3.4)$$

Quantity $v(r_{12})$ is the ${}^4\text{He}$ - ${}^4\text{He}$ interaction potential (Lennard-Jones or Aziz). The two-body functions $g(\eta, z_1, z_2)$, $N(\eta, z_1, z_2)$, and $X(\eta, z_1, z_2)$ are determined by the hypernetted and Ornstein-Zernike chain equations given by Eqs. (2.6)–(2.8) in Ref. 21.

In fact, two series of results were evaluated for coverages ranging from $n_c = 0.04$ to 0.32 \AA^{-2} , one by using the standard 6-12 Lennard-Jones potential and the other by utilizing the Aziz ${}^4\text{He}$ - ${}^4\text{He}$ interaction.⁴⁶ Since in the short-ranged approach there is no infrared divergence one gets very precise numerical results. Both sets of evaluated short-ranged density profiles exhibit similar features to the optimized ones plotted in Fig. 2 of Ref. 7, i.e., a maximum density at the center of the film $\rho_c = \rho(z=0)$ and a smoothly decreasing $\rho(z)$ which falls out at the surfaces. A typical difference between short-ranged and optimized films is displayed in Fig. 5 of Ref. 11. The energy per particle was computed according to

$$\frac{E}{N} = \frac{1}{n_c} \left[\frac{\hbar^2}{2m} \int_{-\infty}^{\infty} dz_1 \left(\frac{d\sqrt{\rho(z_1)}}{dz_1} \right)^2 + \int_{-\infty}^{\infty} \int_{-\infty}^{\infty} dz_1 dz_2 \rho(z_1) \rho(z_2) E_c(z_1, z_2) \right], \quad (3.5)$$

with the correlation energy density $E_c(z_1, z_2)$ given by Eq. (3.3). Figure 1 shows a rather complete pattern of the behavior of the short-ranged values μ and E/N calculated with the Aziz potential. It clearly indicates that both the energy per particle and the chemical potential vanish in the limit of zero coverage, which is a usually required physical feature. In addition, this figure shows that both quantities are monotonically decreasing functions of n_c . After including in Fig. 1 the values of E/N quoted in Table I of Ref. 7 one realizes that the results obtained with improved two-body functions are, as expected, somewhat lower than the short-ranged ones but the trend of both sets is similar. The fact that the short-ranged and optimized values of μ lie on almost parallel curves and that an alike behavior is exhibited by E/N becomes the relevant feature, which gives a strong support to the method of analysis employed in this section.

In order to facilitate a better visual insight when exploring the variation of μ , the main sector of Fig. 1 is amplified in

Fig. 2. Furthermore, the latter picture is completed by including the values of μ obtained with the Lennard-Jones interatomic potential to allow a direct comparison, since such data are only partially listed in Table II of Ref. 11. From this plot it becomes clear that μ always decreases monotonically for increasing coverage and that calculations carried out by adopting the Lennard-Jones and Aziz interactions provide equivalent results. Of course, the latter values are somewhat lower than the former ones as expected for a more realistic potential.⁴⁷

Going ahead with the analysis we shall focus our attention on $n_c(d\mu/dn_c)$. These scaled derivatives evaluated in case of the Aziz potential are shown in Fig. 3(a). Since the slopes calculated by using μ obtained with the Lennard-Jones potential yielded alike negative results to that already displayed in Fig. 3(a), such values are not included therein avoiding the overload of the graph. Figure 3(a) shows that all CBF-HNC/0 values of $n_c(d\mu/dn_c)$ are negative and, in addition,

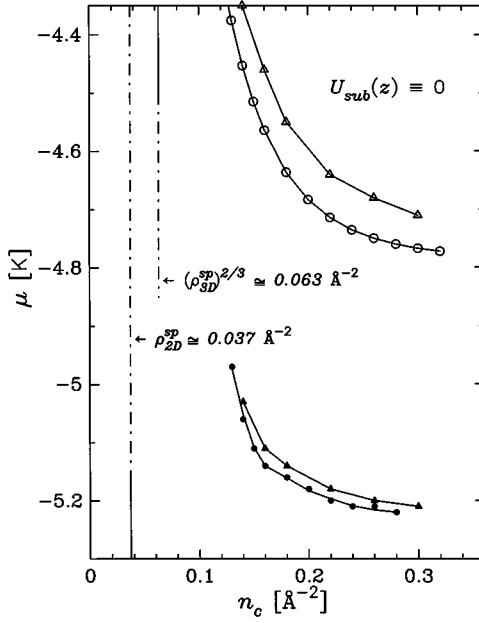


FIG. 2. Chemical potential as a function of the coverage. Circles and triangles represent CBF-HNC/0 evaluations carried out with the Aziz and Lennard-Jones potentials, respectively. Open circles are the short-ranged values calculated in the present work, while full circles stand for the optimized values listed in Table I of Ref. 7. Open and full triangles are, respectively, the short-ranged and optimized values determined in the investigation reported in Ref. 11. The vertical lines indicate the two-dimensional spinodal density ρ_{2D}^{sp} and the equivalent surface density $(\rho_{3D}^{sp})^{2/3}$ of the three-dimensional spinodal value.

it indicates that the short-ranged and optimized results are of the same order of magnitude. A noticeable feature is the pronounced drop of the optimized scaled slopes for coverages below $n_c = 0.18 \text{ \AA}^{-2}$. We think that this behavior of $n_c(d\mu/dn_c)$ is indeed not fortuitous and may be correlated with the low one-body densities obtained for such films. The values of ρ_c taken from Table I of Ref. 7 are plotted in Fig. 3(b). Looking at this figure one realizes that films with $n_c < 0.18 \text{ \AA}^{-2}$ have ρ_c smaller than the three-dimensional spinodal density $\rho_{3D}^{sp} \approx 0.0158 \text{ \AA}^{-3}$, below of which a bulk system does not have a physical solution. Making a connection to results for adsorbed systems it can be noticed that Figs. 10 and 15 of Ref. 17 and Fig. 1 of Ref. 23 show that all stable films with a monolayer, bilayer, or multilayer structure always have an average density larger than ρ_{3D}^{sp} . Therefore, the definitive breakdown of the stability condition for free films with $n_c < 0.18 \text{ \AA}^{-2}$ is to some extent an expected behavior. Figure 3(b) shows that for larger coverages, $n_c > 0.18 \text{ \AA}^{-2}$, the optimized systems have $\rho_c > \rho_{3D}^{sp}$ indicating the existence of a region with $\rho(z) > \rho_{3D}^{sp}$. However, this feature is not sufficient to guarantee stability, it only makes these thicker films less unstable. In summary, it appears that the required n_c^{\min} for a stable geometry is still not reached in the analyzed coverage regime, $n_c \leq 0.30 \text{ \AA}^{-2}$.

2. Chemical potential in the NLDF theory

In order to have an alternative way for evaluating the slope of μ as a function of n_c we have also studied free

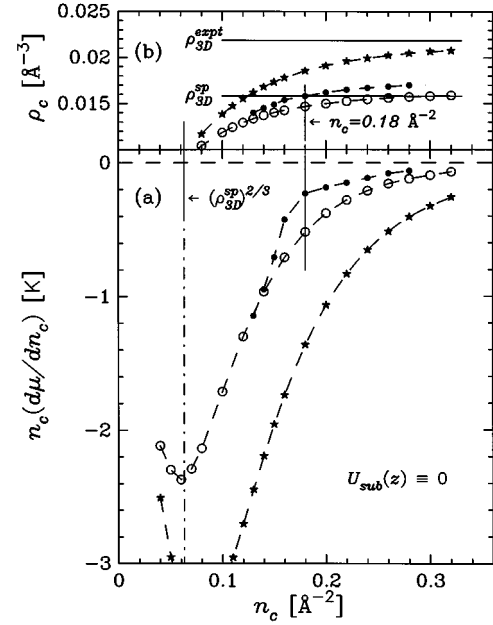


FIG. 3. (a) Scaled derivative of the chemical potential as a function of the coverage. The vertical line indicates the equivalent surface density $(\rho_{3D}^{sp})^{2/3}$ of the three-dimensional spinodal value. (b) Central density of the symmetric film for each coverage. The horizontal lines indicate the values of ρ_{3D}^{sp} and the experimental equilibrium density $\rho_{3D}^{sp, \text{exp}} = 0.02185 \text{ \AA}^{-3}$. In both parts of the figure open and full circles stand, respectively, for short-ranged and optimized CBF-HNC/0 results, while stars are NLDF values.

planar films by applying the NLDF theory. In this approach the density of correlation energy may be written as

$$E_c(z_1, z_2) = \pi \int_0^\infty d\eta \eta v_l(r_{12}) + \frac{c}{2} [\rho(z_2)]^{-1} [\bar{\rho}(z_2)]^{1+\gamma} \times \delta(z_2 - z_1), \quad (3.6)$$

which is in agreement with Eqs. (11a) and (11b) of Ref. 33. Here $v_l(r_{12})$ is the ‘‘screened’’ ^4He - ^4He Lennard-Jones interaction potential (with the standard de Boer–Michels parameters $\epsilon = 10.22 \text{ K}$ and $\sigma = 2.556 \text{ \AA}$)

$$v_l(r_{12}) = \begin{cases} 4\epsilon \left[\left(\frac{\sigma}{r_{12}} \right)^{12} - \left(\frac{\sigma}{r_{12}} \right)^6 \right] & \text{for } r_{12} \geq h, \\ v_l(h) \left(\frac{r_{12}}{h} \right)^4 & \text{for } r_{12} < h, \end{cases} \quad (3.7)$$

where h is the screening distance. The $\bar{\rho}(z_2)$ is the ‘‘coarse-grained density’’ defined by the average of $\rho(z)$ over a sphere of radius h centered at $z = z_2$, see Eq. (10b) of Ref. 33

$$\bar{\rho}(z_2) = \frac{3}{4\pi h^3} \int dr_3 \rho(z_3) \theta(h - r_{23}) = \frac{3}{4h} \int_{z_2-h}^{z_2+h} dz_3 \rho(z_3) \left[1 - \left(\frac{z_3 - z_2}{h} \right)^2 \right]. \quad (3.8)$$

The density correlation energy $E_c(z_1, z_2)$ adopted in the NLDF theory contains much more information about the be-

havior of real liquid ${}^4\text{He}$ than that utilized in the CBF-HNC/0 expansion. It has three free parameters h , c , and γ , which are determined by fitting the equation of state, surface tension, and static density-density response function of bulk ${}^4\text{He}$. In our numerical task we used the values h

$= 2.377 \text{ \AA}$, $c = 1.04554 \times 10^7 \text{ K \AA}^{3(1+\gamma)}$, and $\gamma = 2.8$ given in Ref. 36.

The integrodifferential problem (2.11) was solved for a large domain of coverages by using the NLDF mean-field potential $V_H(z)$ given by expression (2.16) in Ref. 36:

$$V_H(z_1) = 4\pi\epsilon\sigma^2 \left(\int_{-\infty}^{z_1-h} + \int_{z_1+h}^{\infty} \right) dz_2 \rho(z_2) \left[\frac{1}{5} \left(\frac{\sigma}{z_1-z_2} \right)^{10} - \frac{1}{2} \left(\frac{\sigma}{z_1-z_2} \right)^4 \right] + 4\pi\epsilon\sigma^2 \int_{z_1-h}^{z_1+h} dz_2$$

$$\times \rho(z_2) \left\{ \left[\frac{8}{15} \left(\frac{\sigma}{h} \right)^6 - \frac{5}{6} \right] - \frac{1}{3} \left[\left(\frac{\sigma}{h} \right)^6 - 1 \right] \left(\frac{z_1-z_2}{h} \right)^6 \right\} \left(\frac{\sigma}{h} \right)^4 + \frac{c}{2} [\bar{\rho}(z_1)]^{1+\gamma}$$

$$+ \frac{3c}{8h} (1+\gamma) \int_{z_1-h}^{z_1+h} dz_2 \rho(z_2) [\bar{\rho}(z_2)]^\gamma \left[1 - \left(\frac{z_1-z_2}{h} \right)^2 \right]. \quad (3.9)$$

The energy per particle was evaluated using Eq. (3.5) with Eq. (3.6). Results of μ and E/N for films with $n_c \leq 0.32 \text{ \AA}^{-2}$ are displayed in Fig. 1. A glance at this figure indicates that both these quantities tend towards zero in the limit $n_c \rightarrow 0$. For the purpose of this work, it is important to notice that the new values of μ as well as of E/N decrease monotonically for increasing n_c . The NLDF values are lower than the CBF-HNC/0 ones. This feature can be well understood if one reminds the reader that the correlation energy in the NLDF approach contains a large piece of information about properties of bulk ${}^4\text{He}$, while the CBF-HNC/0 calculations only include the lowest-order contributions of the correlation factors. This difference increases for increasing coverage due to the fact that larger films present wider central regions with larger densities and for such systems the higher-order contributions not included in the CBF-HNC/0 expansion are more important. Furthermore, it is worthwhile to point out that for $n_c = 0.30 \text{ \AA}^{-2}$ the NLDF chemical potential, $\mu(0.30) = -6.94 \text{ K}$, is already close to the experimental value of the energy per particle of a uniform system $E_B/N = -7.14 \text{ K}$, the difference only amounts to about 3%. On the other hand, the central densities ρ_c obtained in NLDF calculations are plotted in Fig. 3(b), where one sees that for increasing coverage the results go towards the experimental equilibrium density of the bulk liquid $\rho_{3D}^{\text{expt}} = 0.02185 \text{ \AA}^{-3}$.

It already becomes clear from Fig. 1 that the slope of the chemical potential determined with the NLDF theory is negative. Nevertheless, in order to quantify the effect we evaluated the corresponding values of $n_c(d\mu/dn_c)$. The NLDF scaled slopes displayed in Fig. 3(a) indicate in a very clean way that free planar films with $n_c \leq 0.30 \text{ \AA}^{-2}$ are unstable. These results support the conclusion obtained from CBF-HNC/0 calculations.

C. The limit of very thick films

Let us now refer to the stability of self-supported planar systems with $n_c > 0.30 \text{ \AA}^{-2}$. This part of the investigation is based on NLDF evaluations. The largest solved film has a coverage $n_c = 0.5 \text{ \AA}^{-2}$ and a width of 25 \AA , i.e., it is more

than 10 times wider than a typical interatomic distance $\approx 2 \text{ \AA}$. Measured in nominal ‘layers’

$$\ell = \frac{n_c}{\rho_c^{2/3}} = \frac{1}{\rho_c^{2/3}} \int_{-\infty}^{\infty} dz \rho(z), \quad (3.10)$$

the thickness of this film with $n_c = 0.5 \text{ \AA}^{-2}$ and $\rho_c = 0.02148 \text{ \AA}^{-3}$ is $\ell \approx 6.5$. When looking at thick films it is convenient to examine the data as a function of the inverse of the coverage. Figure 4 shows the corresponding behavior of the chemical potential, energy per particle and surface tension. The latter quantity is equal to half of the free energy per unit area

$$\sigma_s = \frac{1}{2} \frac{E - \mu N}{A} = \frac{1}{2} \left[\frac{E}{A} - \mu n_c \right], \quad (3.11)$$

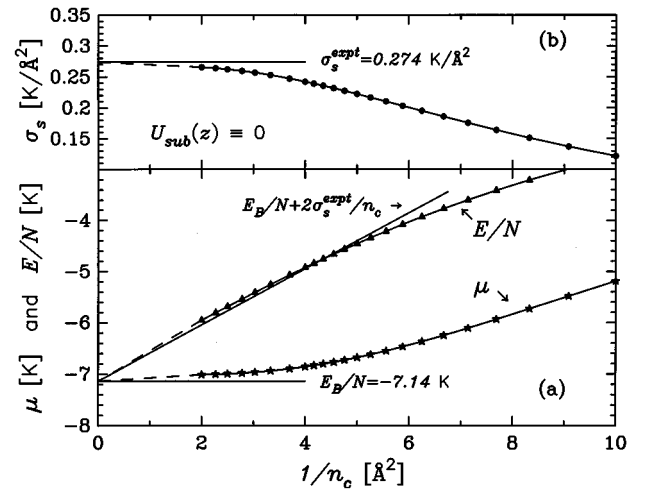


FIG. 4. Chemical potential, energy per particle, and surface tension evaluated according to the NLDF theory as a function of the inverse of the coverage. In the limit $1/n_c \rightarrow 0$ data of μ and E/N approach the experimental value of the energy per particle of a bulk ${}^4\text{He}$ liquid E_B/N , while σ_s tends towards the experimental surface tension σ_s^{expt} . The asymptotic behavior of the energy per particle, i.e., $E_B/N + 2\sigma_s^{\text{expt}}/n_c$ is also indicated.

because a planar film has two equivalent surfaces. In order to study the stability analyzing data of a plot μ vs $1/n_c$ one must consider that condition (2.12) takes the form

$$mc_3^2 = n_c \frac{d\mu}{dn_c} = -\frac{1}{n_c} \frac{d\mu}{d(1/n_c)} > 0. \quad (3.12)$$

This means that stable films require negative values of the slope $d\mu/d(1/n_c)$. However, Fig. 4(a) shows that such a slope is always positive, hence, one concludes that all the calculated films are unstable.

Although we have not carried out calculations for larger coverages, it seems possible to infer the behavior of bigger films with an important degree of confidence. Figure 4 indicates that the results exhibit the following features as $1/n_c$ decreases: (i) the value of μ tends towards the energy per particle of bulk liquid ${}^4\text{He}$ and (ii) the surface tension approaches the experimental surface tension $\sigma_s^{\text{expt}} = 0.274 \text{ K } \text{\AA}^{-2}$. In addition, from Eq. (3.11) one may derive the following relation:

$$\mu_\infty = \lim_{n_c \rightarrow \infty} \mu = \lim_{1/n_c \rightarrow 0} \left[\frac{E}{N} - \frac{2\sigma_s}{n_c} \right] = \lim_{n_c \rightarrow \infty} \frac{E}{N} = \frac{E_B}{N}, \quad (3.13)$$

which implies that the chemical potential and energy per particle must coincide in the limit $1/n_c \rightarrow 0$ and be equal to E_B/N . As far as one can see in Fig. 4(a), the data follow fairly well the trend required by this property. It is also noticeable that the calculated E/N are not far away from the asymptotic behavior given by

$$\left(\frac{E}{N} \right)_{\text{asympt}} = \frac{E_B}{N} + 2\sigma_s^{\text{expt}} \left(\frac{1}{n_c} \right), \quad (3.14)$$

as shown in Fig. 4(a). Perhaps, it is still interesting to discuss a little bit more the way in which the chemical potential may reach its asymptotic value. As is known, the third-sound velocity goes asymptotically to zero in the limit $n_c \rightarrow \infty$.²⁵ Since $n_c(d\mu/dn_c)$ is negative for all the films investigated in the present work, to have a domain of stable coverages such a derivative must cross to positive values. This crossing together with the asymptotic zero value would mean a sort of oscillation of mc_3^2 as a function of n_c . However, as mentioned before, any oscillatory behavior of mc_3^2 is related to a layer formation caused by a compression due to substrate potentials.¹ Since free films are not supported by any external potential, there is no source to produce a belated oscillation of mc_3^2 . Hence, the asymptotic result $mc_3^2 = n_c(d\mu/dn_c) = -(1/n_c)[d\mu/d(1/n_c)] = 0$ would be reached from negative values. In other words, it seems that there is no physical reason to expect a change of the monotonic trend of all the quantities displayed in Fig. 4.

IV. CONCLUSION AND FINAL DISCUSSION

In summary, we conclude that in light of the facts described in this paper there is strong evidence in favor of the instability of the free films of liquid ${}^4\text{He}$ at $T=0 \text{ K}$. Prior to the discovery of the instability effect in confined films, most theoretical physicists were skeptical of the possibility that

free films might be unstable, but in this work we demonstrate that it is possible to join sufficient arguments for changing that viewpoint.

The stability was examined by looking at the third-sound velocity expressed as an energy mc_3^2 . This quantity was evaluated by using the procedures described in Sec. II. The calculations were carried out within the framework of two different approaches, namely the CBF-HNC/0 and NLDF theories. All the evaluations for self-supported systems with coverage $n_c \leq 0.30 \text{ \AA}^{-2}$ yielded negative values of mc_3^2 indicating that the investigated films are unstable. The numerical task in the case of the CBF-HNC/0 expansion is very delicate, since the evaluated $n_c(d\mu/dn_c)$ are small. The values of the latter quantity estimated with optimized data reported in Refs. 7 and 11 and plotted in Fig. 3(a) exhibit an important fall of the stability indicator only for coverages $n_c < 0.18 \text{ \AA}^{-2}$. On the other hand, the NLDF calculations show in a much more clear way that such systems are far from the conditions required by the minimum stable coverage. This finding fits very well in the current knowledge about this matter.¹ It is quite reasonable to expect that, if not very thick films like those studied in Figs. 1–3 are unstable when adsorbed to rubidium and cesium substrates, then such films without a supporting potential should be also unstable.

Although the cohesion increases for larger systems, all the free helium films with $n_c > 0.30 \text{ \AA}^{-2}$ analyzed by using the NLDF theory are still unstable as is shown in Fig. 4. Furthermore, on the grounds of the discussion provided in the text, it is plausible to conjecture that instability would persist for all free films of finite thickness as suggested in Ref. 11. Such a pattern of instability cannot be *a priori* considered unphysical since it is supported by (i) the finding of Refs. 2 and 3 that a free semi-infinite system is unstable and (ii) the nonwetting behavior of liquid ${}^4\text{He}$ on rubidium and cesium surfaces,^{1,45} where besides the steep barrier B/z^9 located near the alkali-metal surface there is an attractive long-ranged van der Waals tail $-C/z^3$ which confines at least weakly the film at the liquid-vacuum interface. Moreover, this phenomenon of instability may be interpreted on the basis of pure physical considerations. Due to the rotational symmetry of the interaction potential between the individual particles, one expects that the ground state of stable free systems of strongly correlated helium atoms, which do not occupy the whole three-dimensional space, will evolve to get rather spherical shapes like those studied in Refs. 48 and 49. This means that such systems will favor the formation of droplets of liquid ${}^4\text{He}$ coexisting with the vacuum. Therefore, in the case of planar films with finite coverage one should apply an external potential with a strong attractive term enough to generate the sufficient compression which could preclude the natural tendency of helium to form spherical clusters.

ACKNOWLEDGMENTS

The author would like to thank John W. Clark and Manfred L. Ristig for valuable discussions. This work was supported by the Ministry of Culture and Education of Argentina through PIP-CONICET Contract No. PMT-PICT0190 and under SIP Grant Nos. 01/X072 and 01/X960.

- *Also at the Carrera del Investigador Científico of the Consejo Nacional de Investigaciones Científicas y Técnicas, Av. Rivadavia 1917, RA-1033 Buenos Aires, Argentina.
- ¹E. Cheng, M. W. Cole, J. Dupont-Roc, W. F. Saam, and J. Treiner, *Rev. Mod. Phys.* **65**, 557 (1993).
 - ²A. Widom, *Phys. Rev. A* **1**, 216 (1970).
 - ³M. W. Cole, *Phys. Rev. A* **1**, 1838 (1970).
 - ⁴J. W. Clark and E. Feenberg, *Phys. Rev.* **113**, 388 (1959).
 - ⁵E. Feenberg, *Theory of Quantum Fluids* (Academic, New York, 1969).
 - ⁶J. W. Clark, in *Progress in Particle and Nuclear Physics*, edited by D. Wilkinson (Pergamon, New York, 1979), Vol. 2, p. 89.
 - ⁷E. Krotscheck, G.-X. Qian, and W. Kohn, *Phys. Rev. B* **31**, 4245 (1985).
 - ⁸E. Krotscheck, *Phys. Rev. B* **31**, 4258 (1985).
 - ⁹E. Krotscheck, *Phys. Rev. B* **32**, 5713 (1985).
 - ¹⁰J. L. Epstein and E. Krotscheck, *Phys. Rev. B* **37**, 1666 (1988).
 - ¹¹L. Szybisz and M. L. Ristig, *Phys. Rev. B* **40**, 4391 (1989).
 - ¹²L. Szybisz, *Phys. Rev. B* **41**, 11 282 (1990).
 - ¹³E. Krotscheck and C. J. Tymczak, *Phys. Rev. B* **45**, 217 (1992).
 - ¹⁴L. Szybisz and R. O. Vallejos, in *Proceedings of the XV International Workshop on Condensed Matter Theories*, Mar del Plata, Argentina, 1991, edited by A. N. Proto and J. L. Aliaga (Plenum, New York, 1992), Vol. 7, p. 107.
 - ¹⁵L. Szybisz, *Z. Phys. B* **90**, 341 (1993).
 - ¹⁶B. E. Clements, E. Krotscheck, and H. J. Lauter, *Phys. Rev. Lett.* **70**, 1287 (1993).
 - ¹⁷B. E. Clements, J. L. Epstein, E. Krotscheck, and M. Saarela, *Phys. Rev. B* **48**, 7450 (1993).
 - ¹⁸B. E. Clements, H. Forbert, E. Krotscheck, and M. Saarela, *J. Low Temp. Phys.* **95**, 849 (1994).
 - ¹⁹B. E. Clements, H. Forbert, E. Krotscheck, H. J. Lauter, M. Saarela, and C. J. Tymczak, *Phys. Rev. B* **50**, 6958 (1994).
 - ²⁰L. Szybisz, *Z. Phys. B* **96**, 235 (1994).
 - ²¹L. Szybisz, *Phys. Rev. B* **53**, 6705 (1996).
 - ²²B. E. Clements, H. Godfrin, E. Krotscheck, H. J. Lauter, P. Leiderer, V. Passioux, and C. J. Tymczak, *Phys. Rev. B* **53**, 12 242 (1996).
 - ²³B. E. Clements, E. Krotscheck, and C. J. Tymczak, *Phys. Rev. B* **53**, 12 253 (1996).
 - ²⁴M. Saarela, P. Pietiläinen, and A. Kallio, *Phys. Rev. B* **27**, 231 (1983).
 - ²⁵E. Krotscheck, S. Stringari, and J. Treiner, *Phys. Rev. B* **35**, 4754 (1987).
 - ²⁶K. A. Gernoth, Ph.D. thesis, Universität zu Köln, Germany, 1990.
 - ²⁷K. A. Gernoth and M. L. Ristig, *Phys. Rev. B* **45**, 2969 (1992).
 - ²⁸K. A. Gernoth, J. W. Clark, G. Senger, and M. L. Ristig, in *Proceedings of the XVI International Workshop on Condensed Matter Theories*, San Juan, Puerto Rico, 1992, edited by L. Blum and F. B. Malik (Plenum, New York, 1993), Vol. 8, p. 195.
 - ²⁹K. A. Gernoth and J. W. Clark, *J. Low Temp. Phys.* **96**, 153 (1994).
 - ³⁰K. A. Gernoth, J. W. Clark, G. Senger, and M. L. Ristig, *Phys. Rev. B* **49**, 15 836 (1994).
 - ³¹W. F. Saam and C. Ebner, *Phys. Rev. Lett.* **34**, 253 (1975).
 - ³²C. Ebner and W. F. Saam, *Phys. Rev. B* **12**, 923 (1975).
 - ³³J. Dupont-Roc, M. Himbert, N. Pavloff, and J. Treiner, *J. Low Temp. Phys.* **81**, 31 (1990).
 - ³⁴N. Pavloff and J. Treiner, *J. Low Temp. Phys.* **83**, 331 (1991).
 - ³⁵E. Cheng, M. W. Cole, W. F. Saam, and J. Treiner, *Phys. Rev. Lett.* **67**, 1007 (1991).
 - ³⁶E. Cheng, M. W. Cole, W. F. Saam, and J. Treiner, *Phys. Rev. B* **46**, 13 967 (1992).
 - ³⁷W. F. Saam, J. Treiner, E. Cheng, and M. W. Cole, *J. Low Temp. Phys.* **89**, 637 (1992).
 - ³⁸E. Cheng, W. F. Saam, M. W. Cole, and J. Treiner, *J. Low Temp. Phys.* **92**, 11 (1993).
 - ³⁹E. Krotscheck, *Phys. Lett. A* **190**, 201 (1994).
 - ⁴⁰C. Carraro and M. W. Cole, *Phys. Rev. B* **46**, 10 947 (1992).
 - ⁴¹P. J. Nacher and J. Dupont-Roc, *Phys. Rev. Lett.* **67**, 2966 (1991).
 - ⁴²K. S. Ketola, S. Wang, and R. B. Hallock, *Phys. Rev. Lett.* **68**, 201 (1992).
 - ⁴³P. Taborek and J. E. Rutledge, *Phys. Rev. Lett.* **68**, 2184 (1992).
 - ⁴⁴J. E. Rutledge and P. Taborek, *Phys. Rev. Lett.* **69**, 937 (1992).
 - ⁴⁵A. F. G. Wyatt, J. Klier, and P. Stefany, *Phys. Rev. Lett.* **74**, 1151 (1995).
 - ⁴⁶R. A. Aziz, V. P. S. Nain, J. S. Carley, W. L. Taylor, and G. T. McConville, *J. Chem. Phys.* **70**, 4330 (1979).
 - ⁴⁷P. A. Whitlock, G. V. Chester, and M. H. Kalos, *Phys. Rev. B* **38**, 2418 (1988).
 - ⁴⁸V. R. Pandharipande, J. G. Zabolitzky, S. C. Pieper, R. B. Wiringa, and U. Helmbrecht, *Phys. Rev. Lett.* **50**, 1676 (1983).
 - ⁴⁹S. A. Chin and E. Krotscheck, *Phys. Rev. Lett.* **65**, 2658 (1990).